

Article

Study on Rheological Properties and Modification Mechanism of Budun Rock Asphalt/Nano-Silica Composite Modified Asphalt

Chaojie Li ^{1,2,3}, Zhenxia Li ³, Tengteng Guo ³, Yuanzhao Chen ^{3,4,*} , Shangwei Jing ³, Jing Wang ³ and Lihui Jin ³¹ Henan Transportation Research Institute Co., Ltd., Zhengzhou 450006, China; lcj13676936229@163.com² Xi'an Changda Highway Engineering Inspection Center Co., Ltd., Xi'an 710064, China³ School of Civil Engineering and Communication, North China University of Water Resources and Electric Power, Zhengzhou 450045, China; zhenxiali2009@ncwu.edu.cn (Z.L.); guotth@ncwu.edu.cn (T.G.); 13782889126@163.com (S.J.); wj@ncwu.edu.cn (J.W.); lihuijin2023@163.com (L.J.)⁴ Henan Province Engineering Technology Research Center of Environment Friendly and High-Performance Pavement Materials, Zhengzhou 450045, China

* Correspondence: cyz740513@ncwu.edu.cn

Abstract: To enhance the high and low-temperature performance of asphalt materials and extend the service life of asphalt pavement, two types of external admixtures, Butonite rock asphalt, and nano-silica are added to the asphalt. By conducting dynamic shear rheological tests and bending creep stiffness tests, the high and low-temperature rheological properties of Budun rock asphalt/nano-silica composite-modified asphalt were evaluated. The distribution of Budun rock asphalt and nano-silica in asphalt was studied using scanning electron microscopy and infrared spectroscopy tests, revealing the synergistic modification mechanism of Budun rock asphalt and nano-silica. The results show that the optimal dosage of Butonite rock asphalt and nano-silica composite-modified asphalt is 25% and 5%, respectively. At this dosage, the rutting factor $G^*/\sin\delta$ of composite-modified asphalt at 82 °C Compared with the matrix asphalt, the frequency main curve of Budun rock asphalt/nano-silica composite-modified asphalt is higher than that of the matrix asphalt and nano-silica-modified asphalt by 4 kPa. The creep modulus S at -18 °C decreases by 117.2 MPa, indicating that the high-temperature performance, low-temperature performance, and temperature sensitivity of Budun rock asphalt/nano-silica composite-modified asphalt are significantly improved compared to the matrix asphalt; The distribution of nano-silica particles in Budun rock asphalt/nano-silica composite-modified asphalt is uniform, and together with Budun rock asphalt, it forms a stable three-dimensional network skeleton structure; Budun rock asphalt/nano-silica composite-modified asphalt has generated new functional groups, and the blending process is mainly based on physical reactions, supplemented by weak chemical reactions.

Keywords: Budun rock asphalt; nano-silica; composite modified asphalt; rheological properties; modification mechanism



Citation: Li, C.; Li, Z.; Guo, T.; Chen, Y.; Jing, S.; Wang, J.; Jin, L. Study on Rheological Properties and Modification Mechanism of Budun Rock Asphalt/Nano-Silica Composite Modified Asphalt. *Coatings* **2024**, *14*, 226. <https://doi.org/10.3390/coatings14020226>

Academic Editor: Andrea Nobili

Received: 28 January 2024

Revised: 6 February 2024

Accepted: 7 February 2024

Published: 14 February 2024



Copyright: © 2024 by the authors. Licensee MDPI, Basel, Switzerland. This article is an open access article distributed under the terms and conditions of the Creative Commons Attribution (CC BY) license (<https://creativecommons.org/licenses/by/4.0/>).

1. Introduction

Nowadays, China's highways have developed relatively well, and various types of roads have emerged in an endless stream. In particular, asphalt pavement has the characteristics of low noise, stable and comfortable driving, and good mechanical properties. Asphalt pavement has become the most prevalent type of road surface; however, with its widespread use, the load on the pavement is also steadily increasing. Especially for highways and heavy-duty traffic roads, it is easy to have quality problems such as rutting, cracks, and water damage, which also tests the performance of pavement materials [1]. Ordinary asphalt obviously cannot meet the needs of the increasing load of the highway, so modified asphalt came into being. There is a wide range of choices for the incorporation of materials in modified asphalt, and numerous studies have been conducted in this field. The incorporation of each modifier can enhance the specific characteristics of asphalt

to some degree [2,3]. The incorporation of nanomaterials can significantly improve the comprehensive characteristics of asphalt [4]. Nano-silica has the characteristics of abundant reserves, high chemical purity, easy production, and low price. Its extensive utilization extends to various domains, encompassing antibacterial materials, plastic coatings, optics, electronic assembly materials, and other fields [5]. At present, the application of nano-silica-modified asphalt can significantly improve the high and low-temperature properties of asphalt and anti-ultraviolet properties [6–8]. Buton rock asphalt (BRA) is a kind of material with abundant reserves and can greatly improve the high-temperature performance of asphalt mixture [9,10]. Utilizing both nano-silica and Buton rock asphalt as modifiers can more effectively harness their individual enhancing properties. This approach holds considerable importance for the field of pavement engineering, particularly in regions with high temperatures and roads subjected to heavy traffic loads. The use of these two materials to modify asphalt is aimed at improving its performance, prolonging road service life, and alleviating the pressure of petroleum energy shortage and environmental pollution, in line with the global concept of green, environmental protection, and sustainable development.

Many scholars have conducted related research on Buton rock asphalt-modified asphalt mortar. Zhang, Z [11] determined the basic properties of BRA-modified asphalt with 10%, 15%, 20%, 25%, and 30% BRA blending ratios. Research has revealed that as the proportion of Buton rock asphalt (BRA) in the mix is elevated, the high-temperature capabilities of the modified asphalt improve, whereas its performance at lower temperatures tends to diminish, with durability remaining relatively unchanged. Zhihai, Z [12] and Li, R.X et al. [13] determined the basic properties, viscosity, and high and low-temperature rheological properties of various quantities of Buton rock-modified asphalt. The research findings showed that the incorporation of Buton rock asphalt (BRA) resulted in reduced asphalt penetration, elevated softening point, increased viscosity, increased high-temperature PG grade, increased rutting factor, and a slight reduction in the low-temperature performance of asphalt. Muhammad, K et al. [14] used the UTM25 testing machine to conduct dynamic creep tests on unmodified asphalt and BRA-modified asphalt with 10%, 20%, and 30% BRA blending ratios. The enhanced performance of BRA-modified asphalt was observed, and an additional benefit was noted: an increase in BRA content led to a reduction in the overall permanent strain of the asphalt. Bo, S [15] conducted conventional performance tests and rheological performance tests on the high viscosity elastic restored asphalt with different modifier content, and the research showed that the rutting factor of the modified asphalt with Butunite was significantly improved, that is, Butunite enhanced the high-temperature stability and shear resistance of the asphalt. Yuanfeng, W et al. [16] conducted the high-temperature performance of Buton rock-modified asphalt by conventional test, dynamic shear rheological test, and viscosity test. As the Buton rock asphalt content increased, there was a noticeable enhancement in the high-temperature performance of the modified asphalt, as observed by researchers. In addition to directly incorporating BRA into asphalt, Ming, W et al. [17] extracted the ash in BRA to prepare ash mortar, studied the rheological properties through dynamic rheological properties test, and observed the microscopic by the means of infrared spectroscopy and scanning electron microscope. Compared with mineral powder mortar, they found that BRA ash mortar had better high-temperature rheological properties, and the high-temperature grade was 76 °C. At the same time, BRA can increase the adsorption capacity of the filler to the asphalt. In their research, Chuanming, Z et al. [18] prepared BRA-modified asphalt mortar by substituting mineral powder with BRA at levels of 50%, 75%, and 100%, maintaining a powder-to-binder ratio of 1:2. The three indicators, namely asphalt properties, cloth viscosity, and DSR test results, collectively indicated an enhancement in both the high-temperature performance and temperature sensitivity of asphalt mortar, accompanied by an increase in viscosity. Fourier out-of-line spectroscopy and scanning electron microscopy tests found that there was a physical combination between BRA and asphalt mortar, and the mortar interface was improved. Mingchen, L et al. [19] prepared modified asphalt mortar according to different high ash rock asphalt substitution ratios according to the powder-binder ratio of 1:2 and designed a BRAC-16 asphalt mixture.

The mixture satisfies the requirements for road application in cold regions, boasting exceptional performance in high and low temperatures, as well as remarkable water stability. Under a powder-binder ratio of 1:2, Yong, Y et al. [20] formulated an AC-25 asphalt mixture with varying replacement ratios of high ash rock asphalt. The mixture's water stability and high-temperature performance were both significantly enhanced. The modification mechanism was examined using scanning electron microscopy (SEM) and fluorescence microscopy. The analysis revealed that high ash rock asphalt exerted a modifying effect on the asphalt mortar interface.

Currently, scholars have conducted studies on asphalt modification with single nano-silica. Shafabakhsh, G et al. [6] examined the impact of nano-SiO₂ on asphalt cracking at temperatures of −5 °C, −15 °C, and −25 °C, employing the semi-circular bending test (SCB) with mixed mode I/II loading. The results show that nano-SiO₂ increases the maximum stress intensity factor (SIF) in asphalt. When the content of SiO₂ is 1.2%, the critical stress intensity molecules of the cracked sample are significantly improved, and the low-temperature performance of asphalt is enhanced. Gholam, A.S. et al. [21] used direct shear rheometer and multi-stress creep recovery to conduct rheological tests on nano-SiO₂-modified asphalt. The results revealed that, at 40 °C, the fatigue life of 1.2% nano-SiO₂-modified asphalt increased by 50% compared to the matrix asphalt. Additionally, the rutting resistance showed a 100% increase, signifying that the inclusion of nano-SiO₂ effectively enhanced the rheological properties of the asphalt. Lu, S et al. [22] investigated the rheological properties and road performance of nano-SiO₂-modified asphalt with different contents by DSR, BBR, and road performance tests. The findings indicate that nano-SiO₂ can significantly enhance the high-temperature flow characteristics of asphalt, with a more pronounced effect observed at lower frequencies. Wenxia, Z [23] The effect of nano-SiO₂ on the low-temperature crack resistance, fatigue performance, and rutting resistance of modified asphalt mixture with 0.5%~6.0% nano-SiO₂ was obtained by differential scanning calorimetry and thermal gravimetric analysis. Lu, S et al. [24] conducted a road performance test on nano-SiO₂-modified asphalt mixture, revealing that nano-SiO₂ significantly improved the high-temperature stability and water stability of the asphalt mixture. Yang, Y.S [25] studied the viscosity of nano-SiO₂-modified asphalt emulsion. The results indicated a decline in both penetration and ductility of the modified asphalt emulsion, with a simultaneous rise in viscosity corresponding to the increase in nano-SiO₂ content. Mehmet, S et al. [26] prepared 0.1%, 0.3%, and 0.5% nano-SiO₂-modified asphalt, measured the rutting resistance and fatigue properties of asphalt, and observed the distribution of nanoparticles by scanning electron microscopy. The investigation revealed that at a SiO₂ content of 0.3%, the asphalt's performance exhibited more pronounced improvement, with agglomeration degrees of less than 4 μm and uniform distribution. He, H. et al. [27] considered that the agglomeration of nanoparticles (NPs) in nano-SiO₂-modified asphalt was serious, so the solvent SiO₂ nanofluids (NFs) were incorporated into the asphalt for modification. The investigation into the thermal stability of the asphalt employed various techniques such as scanning electron microscopy, Fourier transform infrared spectroscopy, thermogravimetric analysis, and dynamic shear rheology. The results suggest a consistent dispersion of nanofluids throughout the asphalt system. The incorporation of SiO₂ (NFs) notably improves the resistance of the asphalt mixture to low-temperature cracking and fatigue, with only a minimal adverse effect on high-temperature stability. Chuang, Y et al. [28]. first chemically modified the matrix asphalt, and then added SiO₂ grafted with polyethylenimide to prepare high-performance modified asphalt. The test found that the prepared modified asphalt had better dispersion, chemical reaction and physical reaction with asphalt, and high temperature and anti-aging properties were improved. Yanqing, T [29] used oil-wet nano-SiO₂ to observe the microstructure of oil-wet nano-SiO₂ and asphalt by SEM and to study the influence of oil-wet nano-SiO₂ and matrix asphalt on temperature sensitivity and rheological properties. The findings indicate that the modified asphalt demonstrates superior aging resistance and rheological properties. Henglong, Z et al. [30] discovered enhanced compatibility between asphalt and surface-modified nano-

SiO₂ through physical properties testing of asphalt and high-temperature storage stability testing under ultraviolet aging conditions. Meanwhile, Long, Z. et al. [31,32] unveiled the compatibility principle between nano-SiO₂ and asphalt using molecular dynamics (MD). The compatibility of nano-SiO₂ with saturates surpasses that with asphaltenes. The incorporation of nano-SiO₂ restrains the volatilization of saturates within asphalt, facilitating increased diffusion of saturates. This accelerated diffusion rate of distinctive structural molecules within the asphalt fosters self-healing and augments asphalt durability. Rezaei, S et al. [33] measured the high-temperature performance of nano-SiO₂/SBS composite-modified asphalt, which showed that the high-temperature performance of asphalt was significantly improved. Abed, A.H. et al. [34] conducted FTIR analysis of 3% and 5% nano-SiO₂/SBS composite-modified asphalt and found that the composite-modified asphalt had better oxidation resistance than the matrix asphalt. Mostafa, S. et al. [35] analyzed the road performance of SMA-type nano-SiO₂/TiO₂ composite-modified asphalt mixture, and the results showed that the mechanical properties of SMA asphalt mixture could be improved by adding nano-SiO₂. Shafabakhsh, G. H. et al. [36] prepared composite modified steel slag asphalt mixture mixed with nano-SiO₂ and nano-TiO₂. By studying the rheology of modified asphalt, it was found that the addition of nano-SiO₂ and TiO₂ increased the toughness and viscosity of asphalt by 30% and 109%, respectively, and the permeability grade of asphalt decreased.

Taking into account the research status, it has been demonstrated that incorporating Buton rock asphalt into asphalt enhances its high-temperature performance and temperature sensitivity. The impact is more pronounced with an increased blending ratio of Buton rock asphalt, and it has a less significant effect on the low-temperature performance of asphalt. Additionally, the inclusion of nano-silica in asphalt proves effective in improving its performance across high and low temperatures, water stability, and rheological properties, albeit with an associated increase in asphalt viscosity. Drawing upon the research conducted by scholars both domestically and internationally regarding Buton rock-modified asphalt and nano-silica-modified asphalt, it is noteworthy that Buton rock asphalt exhibits a substantial capability to enhance the high-temperature performance and fatigue resistance of asphalt. Nevertheless, its influence on the low-temperature performance of asphalt is relatively subdued. Nano-silica exhibits a notable capability to improve the low-temperature performance of asphalt. However, its effectiveness in enhancing high-temperature performance does not match the demonstrated efficacy of Buton rock asphalt. The modification effect of a single modifier on asphalt is not as good as that of the composite modifier. Hence, this study opts for Buton rock asphalt and nano-silica as modifiers to formulate a composite-modified asphalt. It comprehensively examines high-temperature rheological properties, low-temperature performance, and the modification mechanism. The aim is to achieve a composite-modified asphalt exhibiting exceptional high and low-temperature performance.

2. Raw Materials

2.1. Asphalt

The 70# matrix asphalt was used for experiments, and its technical indicators were tested according to specifications. The test results are shown in Table 1.

Table 1. Basic performance index of asphalt.

Item	Unit	Result	Specification
needle penetration (25 °C, 100 g, 5 s)	0.1 mm	60.7	60~80
ductility (5 °C, 5 cm/min)	cm	11.3	≥0
softening point	°C	46.9	≥46
penetration index PI		−0.49	−1.5~+1.0
equivalent softening point	°C	50.66	actual measurement
equivalent brittle point	°C	−14.87	actual measurement
	Rotating film residue (163 °C, 85 min)		
rate of quality-led loss	%	0.41	−0.8~+0.8
ductility (5 °C)	cm	7.8	≥6
penetration ratio (25 °C)	%	70.9	≥61

2.2. Buton Rock Asphalt

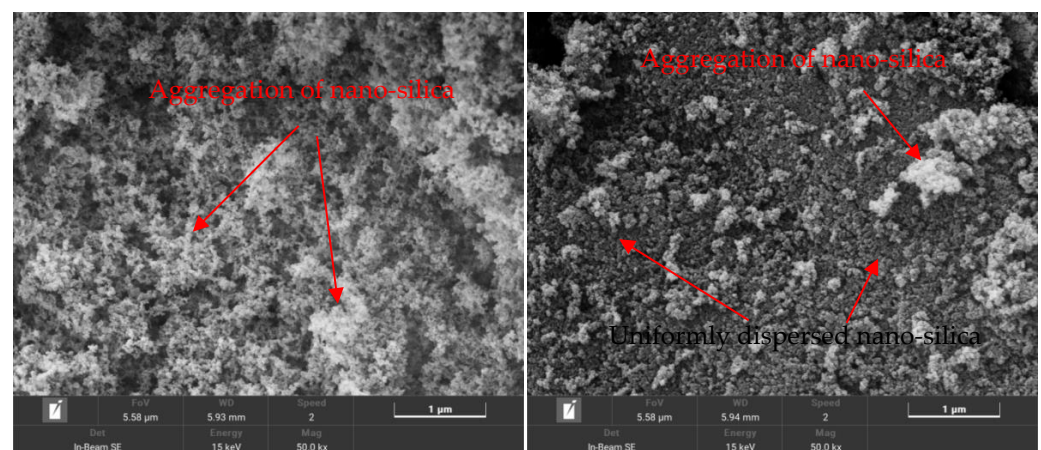
The experiment selected Indonesian high ash rock asphalt (BRA) produced by Indonesia Budun Rock Asphalt Co., Ltd. (BAI) (Nicaea, India) and sold by Anhui Zhongyin Natural Rock Asphalt Technology Co., Ltd. (Anhui, China) Budun rock is composed of 27.2% asphaltene and 72.8% limestone minerals. The main technical indicators are shown in Table 2 and meet the requirements of the specification [37].

Table 2. Technical indicators of Butun rock asphalt.

Item	Unit	Result	Specification
mass fraction of asphalt	%	27.2	≥ 25
density	g/cm^3	1.77	1.60~1.80
water content	%	0.96	≤ 2
loss on heating	%	0.62	≤ 2
maximum particle size	mm	1.18	-
solubility	%	24.3	≥ 18

2.3. Nano-Silica

Nano-silica (nano-SiO₂) is an inorganic chemical material, also known as white carbon black. It is non-toxic, odorless, and pollution-free. It is a spherical microstructure and insoluble in organic solvents. The nano-SiO₂ of Hubei Huifu Nanomaterial Co., Ltd. (HL-200 type) was used in the test. In this study, a 5% silane coupling agent KH-550 is chosen to initially modify the surface of nano-silica, ensuring excellent compatibility with asphalt. The microscopic test images of silica before and after surface modification are shown in Figure 1. Microscopic scanning electron microscopy was used to observe the dispersion state of surface-modified nano SiO₂ particles, and it was found that the agglomeration phenomenon of surface-modified nano SiO₂ was significantly reduced. Silane coupling agent KH-550 was employed to modify the surface of nano SiO₂, effectively reducing the surface energy of nanomaterials. This process aimed to facilitate better integration and even dispersion of nano SiO₂ within the asphalt. The principal technical parameters are illustrated in Table 3. The utilized nano-silica adheres to the specification's stipulations [38].



(a)

(b)

Figure 1. Electron microscopy images of nano-silica before and after treatment were magnified by 50,000 times. (a) Untreated nano-silica magnified by 50,000 times; (b) Surface-modified nano-silica magnified by 50,000 times.

Table 3. Technical indicators of nano-SiO₂.

Item	Unit	Result	Specification
appearance		white powder	white powder
purity	%	99.84	≥99.8
mean diameter	nm	20	-
specific surface area	m ² /g	217	200 ± 20
Suspension pH value		4.15	3.9~4.5
105 °C volatiles	%	0.46	≤2.0
ignition loss	%	0.47	≤2.0
tap density	g/L	52	40~60
45 μm sieve residue	mg/kg	30	≤250

By observing the dispersion state of nano SiO₂ particles before and after treatment through microscopic scanning electron microscopy, it can be seen from Figure 1a that untreated nano SiO₂ exhibits severe agglomeration, which is due to the extremely small particle size, large specific surface area, and high surface energy of nano SiO₂ itself. When untreated nano SiO₂ is added to asphalt, it is easy to cause adverse modification phenomena such as nano-material agglomeration, difficulty in addition, and separation after addition. As shown in Figure 1b, the agglomeration phenomenon of surface-modified nano SiO₂ is significantly reduced. The use of silane coupling agent KH-550 for surface modification of nano SiO₂ eliminates the surface energy of the nano-material, allowing nano SiO₂ to better integrate and uniformly disperse in asphalt. It can be seen that the agglomeration phenomenon of surface-modified nano SiO₂ is significantly reduced. The use of silane coupling agent KH-550 for surface modification of nano SiO₂ eliminates the surface energy of the nano-material, allowing nano SiO₂ to better blend and uniformly disperse in asphalt.

3. Experimental Scheme

3.1. Preparation of Buton Rock Asphalt/Nano-Silica Composite-Modified Asphalt

After reading a large number of relevant literature and previous systematic experimental tests, it was found that after adding SiO₂ to the matrix asphalt, the penetration of the modified asphalt decreased, the ductility increased, the softening point increased, the penetration index increased, the equivalent softening point increased, and the equivalent brittle point decreased, and the “inflection point” appeared at the dosage of 5%, indicating that the modification effect of SiO₂ was the best at this concentration. After more than 5%, the performance of modified asphalt will decrease. The content of Budun rock asphalt should not be too high. The high-temperature performance of composite-modified asphalt is the best at a 25% content, while the low-temperature performance can be met. Therefore, 20%, 25%, and 30% are selected for composite modification. The preparation process of Budun rock asphalt/nano-silica composite-modified asphalt is as follows:

- (1) Heat the base asphalt to a molten state and maintain it at 160 °C, pour nano SiO₂ into the base asphalt, and mix it with a glass rod. After pouring all, manually mix for 30 min.
- (2) Cut at a speed of 5500 r/min for 20 min at high speed, pour the designed amount of Burton rock asphalt into the asphalt, and cut at high speed for 30 min at a speed of 5500 r/min.
- (3) Place the sheared composite-modified asphalt in a 170 °C oven to swell for 20 min, then mix it appropriately with a glass rod to remove any bubbles in the composite-modified asphalt, thus completing the preparation of the composite-modified asphalt.

3.2. Dynamic Shear High-Temperature Rheological Test

In contrast to traditional performance measures like penetration, ductility, and softening point, the dynamic mechanical performance index reflects the viscoelastic alterations of asphalt during real-world usage. As a representative viscoelastic material, asphalt’s viscoelasticity is temperature-dependent, with its dynamic mechanical attributes encompass-

ing alterations in viscosity and elasticity. It is imperative to assess the dynamic mechanical property variations of asphalt across the designated temperature spectrum.

The instrument used in the shear rheological test in this paper is the DHR-1 dynamic shear rheometer manufactured by TA Instruments in the United States. Based on recommendations and requirements from experience and standards [38], determine the Buton rock asphalt/nano-silica composite-modified asphalt DSR temperature scanning test, with a temperature range of 46–82 °C, interval 6 °C (46 °C, 52 °C, 58 °C, 64 °C, 70 °C, 76 °C, 82 °C) scanning, test process control 10 rad/s loading frequency, and 10% strain level. The sample dimensions are 25 mm in diameter and 2 mm in thickness. By means of the DSR temperature scanning test, the variation pattern of the complex shear modulus G^* and phase angle δ is derived as the temperature is incrementally raised based on the designated intervals. Rutting factor $G^*/\sin\delta$ represents high-temperature rutting resistance, and the higher the value, the better the high-temperature rutting resistance. The rutting factor $G^*/\sin\delta$ is calculated, facilitating the development of a relationship curve depicting the correlation between the rutting factor and temperature. This analysis serves to assess the asphalt's temperature stability. Through the DSR frequency scanning test, five different temperature environments were selected to evaluate the frequency changes of five kinds of asphalt, and the main curve was drawn to further expand the temperature range for analysis. The multi-stress creep recovery test involves calculating the average strain recovery rate (R) and the irreversible creep compliance (J_{nr}) based on 20 creep cycles.

3.3. Low Temperature Bending Creep Stiffness Test

With the aim of examining whether the low-temperature performance of Buton rock asphalt/nano-silica composite-modified asphalt surpasses that of matrix asphalt, a low-temperature bending creep stiffness (BBR) test was conducted. The instrument used in this paper is the ATS low-temperature bending beam rheometer of the United States. Based on recommendations and requirements from experience and standards [38], it is determined that the BBR test of Buton rock asphalt/nano-silica composite-modified asphalt is carried out at -12 °C, -18 °C, and -24 °C. Through the BBR test, the stiffness modulus S and the rate of creep stiffness change m were derived, enabling an analysis of the low-temperature crack resistance of the composite-modified asphalt.

3.4. Fourier Infrared Spectroscopy Test

The instrument used in the Fourier transform infrared spectroscopy experiment is the NicolletiS10 Fourier transform infrared spectrometer. Infrared spectroscopy experiments were conducted on matrix asphalt and Budun rock asphalt/nano-silica composite-modified asphalt with a scanning range of 7800 – 375 cm^{-1} , a resolution of 0.4 cm^{-1} , and 64 scanning times.

3.5. Scanning Electron Microscope

The scanning electron microscope experiment was conducted using the JSM-7500F field emission scanning electron microscope. Microscopic observations were conducted on the matrix asphalt and Budun rock asphalt/nano-silica composite-modified asphalt. Firstly, the sample was fixed on the stage with conductive adhesive, and then vacuum gold spraying was performed. After completion, the observation was waited for.

4. Results and Analysis

4.1. Dynamic Shear Test (DSR)

(1) Temperature scanning

DSR tests were carried out on five groups of samples, including matrix asphalt, nano-SiO₂-modified asphalt with 5% content, and Buton rock asphalt-modified asphalt with 5% nano-SiO₂ composite content of 20%, 25%, and 30%, respectively. The complex shear modulus-temperature curve, phase angle-temperature curve, and rutting factor-temperature curve are illustrated in Figures 2–4, respectively.

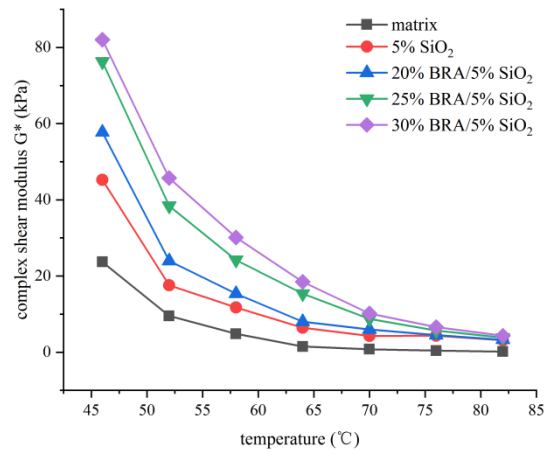


Figure 2. Complex modulus test results.

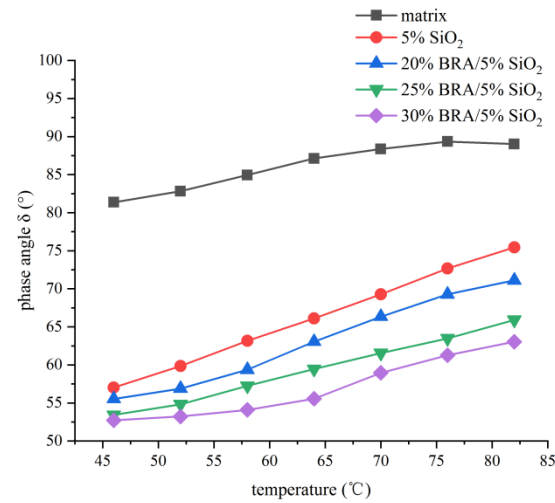


Figure 3. Phase Angle test results.

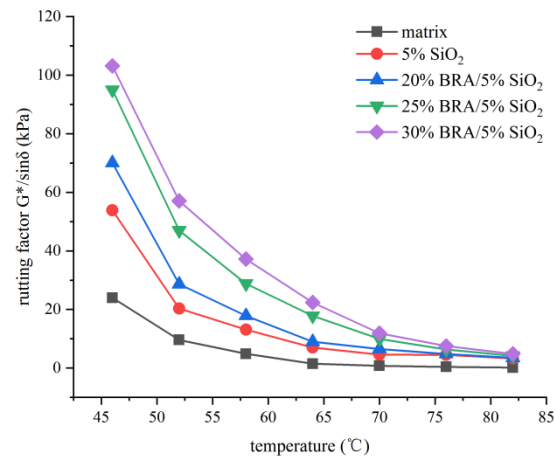


Figure 4. Rutting factor–temperature curve.

Analysis results can be obtained:

The G^* trend for nano-SiO₂-modified asphalt and BRA/nano-SiO₂ composite-modified asphalt shows a decline as temperature increases. At the same temperatures, the G^* of BRA/nano-SiO₂ composite-modified asphalt is notably higher than that of matrix asphalt. The shear resistance of BRA/nano-SiO₂ composite-modified asphalt surpasses that of both

matrix asphalt and nano-SiO₂-modified asphalt. Furthermore, the G^* of the composite-modified asphalt increases proportionally with the augmentation of Buton rock asphalt content. The G^* of the composite-modified asphalt reaches its peak at the same temperature when the Buton rock asphalt content is 30% and the nano-SiO₂ content is 5%. At this time, the shear resistance is the best. Compared with 25% BRA/5% SiO₂ composite-modified asphalt, the G^* by 5.79 kPa at 46 °C, 7.3 kPa at 52 °C, 5.9 kPa at 58 °C, 3.14 kPa at 64 °C, 1.43 kPa at 70 °C, 0.91 kPa at 76 °C, and 0.5 kPa at 82 °C. The findings reveal a consistent enhancement in shear resistance for Buton rock asphalt/nano-silica composite-modified asphalt as the content of Buton rock asphalt increases.

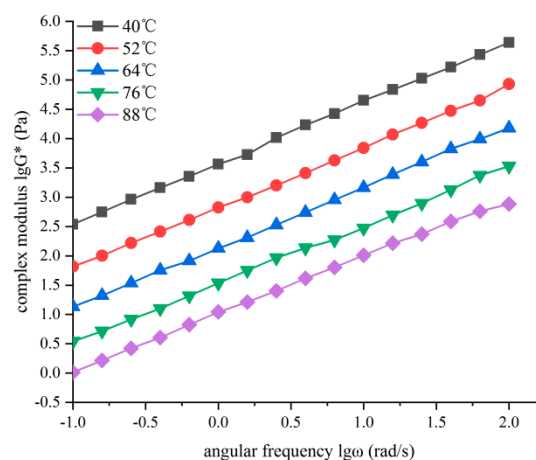
The phase angle of nano-SiO₂-modified asphalt and BRA/nano-SiO₂ composite-modified asphalt gradually increases with rising temperature. At equivalent temperatures, the phase angle of composite-modified asphalt is smaller compared to nano-SiO₂-modified asphalt. This suggests that the addition of Buton rock asphalt has a tendency to decrease the phase angle of the asphalt. At lower temperatures, the phase angle differences among various dosages of composite-modified asphalt are relatively minimal, but these differences become more pronounced as the temperature increases. The composite-modified asphalt exhibits its smallest phase angle when the Buton rock asphalt content is 30% and the nano-SiO₂ content is 5%. The incorporation of Buton rock asphalt and nano-silica increases the viscous component/elastic component in the asphalt and contributes to the deformation recovery of the asphalt.

As the temperature rises, the rutting factor $G^*/\sin\delta$ of the matrix asphalt is 0.77 kPa at 70 °C, and the rutting factor of the original asphalt is required to be ≥ 1.0 kPa in the specification. Compared with 5% nano-SiO₂-modified asphalt, 20%, 25%, and 30% composite-modified asphalt with 5% nano-SiO₂, the rutting factors $G^*/\sin\delta$ at 82 °C are 3.23 kPa, 3.46 kPa, 4.17 kPa, and 4.84 kPa, respectively, which are greater than the specification requirements. This significantly improves the asphalt's resistance to rutting and enhances its high-temperature performance.

Based on the aforementioned analysis, it is evident that the integration of Buton rock asphalt and nano-silica enhances the shear resistance of asphalt, and significantly improves the rutting resistance and high-temperature performance.

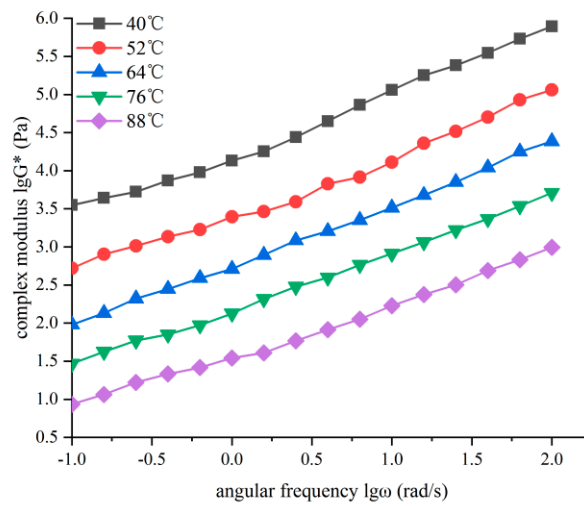
(2) Frequency scanning

The complex modulus of matrix asphalt, 5% nano-SiO₂-modified asphalt, 20%, 25%, and 30% Buton rock asphalt composite 5% nano-SiO₂ composite-modified asphalt was studied at 40 °C, 52 °C, 64 °C, 76 °C, and 88 °C, respectively. The law of change with frequency (0.1–100 rad/s). In the test, the strain level was controlled to 1%, and the complex modulus–angular frequency diagram was drawn as shown in Figure 5.

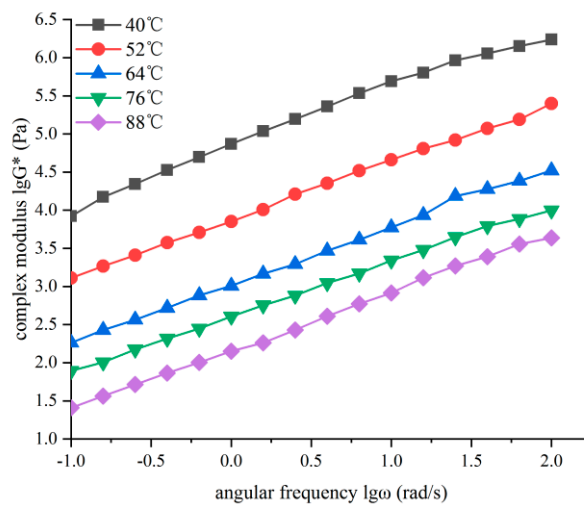


(a) asphalt

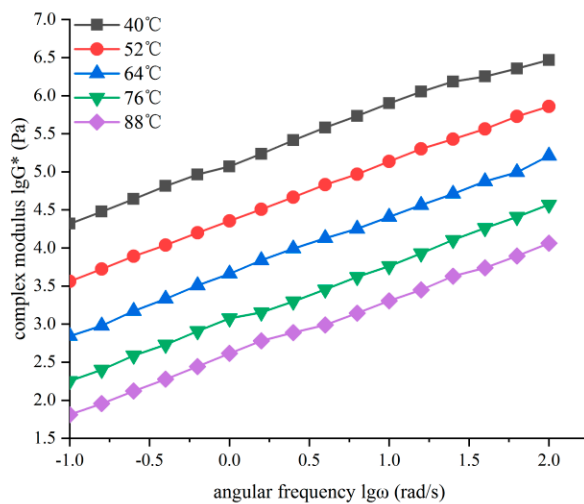
Figure 5. Cont.



(b) 5% nano-SiO₂-modified asphalt.

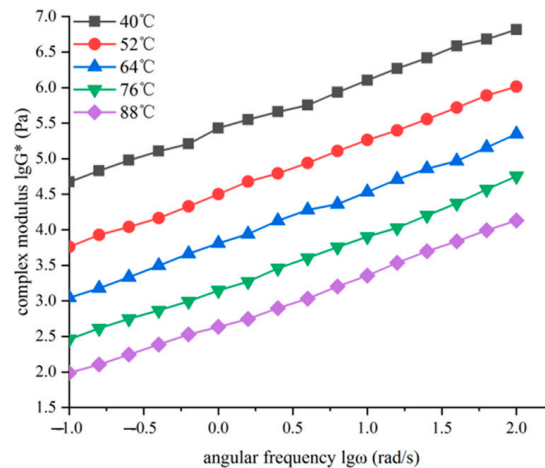


(c) 20% BRA/5% nano-SiO₂ composite-modified asphalt.



(d) 25% BRA/5% nano-SiO₂ composite-modified asphalt.

Figure 5. Cont.



(e) 30% BRA/5% nano-SiO₂ composite-modified asphalt.

Figure 5. Five kinds of asphalt complex modulus change curves.

Analysis results can be obtained: Upon examining Figure 5, it becomes evident that at a constant temperature, the complex modulus of the five asphalt varieties rises in tandem with an increase in angular frequency. This observation signifies that during the practical utilization of asphalt pavement, the vibration duration at a specific asphalt point diminishes as vehicle load speed increases. When the frequency of vehicle load increases, the number of vibrations also increases. The escalation in the frequency of vibrations within specific timeframes results in reduced strain within the asphalt, thereby contributing to a reduction in pavement deformation. At the temperatures of 40 °C, 52 °C, 64 °C, 76 °C, and 88 °C, the slope depicting the alteration in asphalt's complex modulus remains relatively consistent. Furthermore, at identical angular frequencies, the complex modulus of asphalt diminishes with escalating temperatures. This shows that when the temperature increases, the asphalt softens, and the asphalt is a typical viscoelastic material, in which the viscous material increases, the elastic material content decreases, and the external performance is more viscous. In the practical context of asphalt pavement, it can be observed that as asphalt temperature increases, its resistance to deformation diminishes, consequently leading to a decline in high-temperature performance.

Compared with the complex modulus G^* value of different BRA content in the single-doped nano-SiO₂-modified asphalt group, at the same frequency and temperature, with the increase of BRA content, the complex modulus value gradually increases, and at the angular frequency of 0.5 rad/s, at 40 °C, the complex modulus value of the composite-modified asphalt with 30% BRA content is 46.65% higher than that of the matrix asphalt, 30.80% higher than that of the single-doped nano-SiO₂-modified asphalt, and 9.21% higher than that of the composite asphalt with 20% BRA; it is 3.83% higher than that of composite asphalt with 25% BRA. When the temperature reaches 88 °C, the complex modulus value of composite-modified asphalt with 30% BRA content is more than 20% higher than that of single-doped nano-SiO₂-modified asphalt, indicating that BRA plays a more prominent role in improving the high-temperature stability of modified asphalt than single-doped SiO₂ modified asphalt.

(3) Main curve analysis of frequency scanning results

By calculating displacement factors from fitting curves of five asphalt varieties at different temperatures, the primary curve is formed using the time–temperature equivalence principle. This construction aims to broaden the frequency range of the analysis.

(1) Determination of displacement factor

Initially, the frequency scanning outcomes of the matrix asphalt are subjected to curve equation fitting, and the resultant findings are presented in Table 4.

Table 4. Matrix asphalt double logarithm fitting curve equation table.

Testing Temperature (°C)	Curve-Fitting Equation	R ²
40	$\lg G^* = 0.92802 \lg \omega + 3.57715$	0.99941
52	$\lg G^* = 0.92439 \lg \omega + 2.82507$	0.99437
64	$\lg G^* = 0.88651 \lg \omega + 2.12896$	0.99782
76	$\lg G^* = 0.87613 \lg \omega + 1.53576$	0.99924
88	$\lg G^* = 0.87822 \lg \omega + 0.98216$	0.99291

In this paper, $G^* = 1$ kPa, that is, $\lg G^* = 3$, is substituted into the fitting curve equation of Table 4, and the value of $\lg \omega$ is obtained. Taking 40 °C as the reference temperature, the displacement factor is obtained. The findings are displayed in Table 5.

Table 5. Summary of matrix asphalt displacement factors.

Testing Temperature (°C)	$\lg \omega$ ($G^* = 1$ kPa, rad/s)	Shift Factors
40	−0.6219	0
52	0.1892	−0.8111
64	0.9825	−1.6044
76	1.6713	−2.2932
88	2.2976	−2.9195

Likewise, curve fitting equations and displacement factors for nano-SiO₂-modified asphalt and Buton rock asphalt/nano-silica composite-modified asphalt were computed individually. The outcomes are detailed in Tables 6 and 7.

Table 6. Summary of double logarithm fitting curve of modified asphalt.

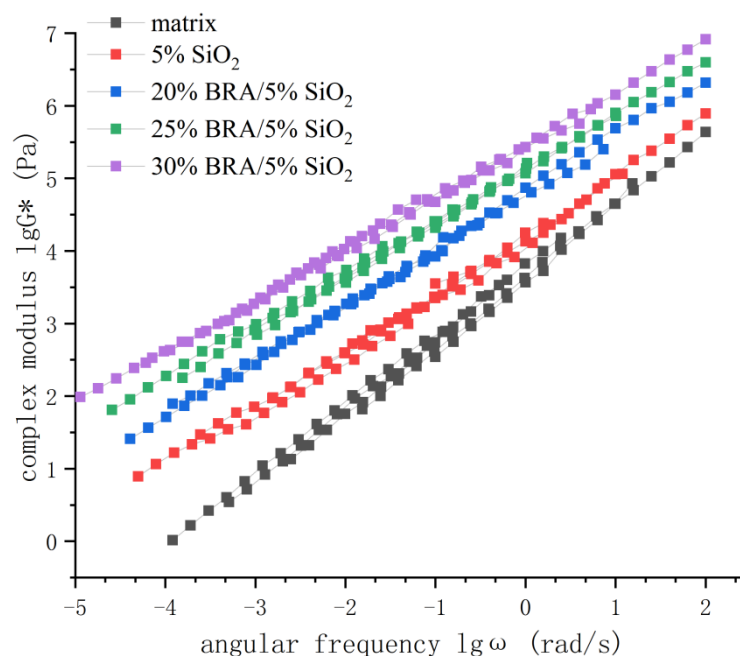
Types of Modified Asphalt	Testing Temperature (°C)	Curve-Fitting Equation	R ²
5% nano-SiO ₂ -modified asphalt	40	$\lg G^* = 0.78164 \lg \omega + 4.13153$	0.99475
	52	$\lg G^* = 0.75020 \lg \omega + 3.39531$	0.99631
	64	$\lg G^* = 0.80127 \lg \omega + 2.71575$	0.99243
	76	$\lg G^* = 0.74692 \lg \omega + 2.13072$	0.99672
	88	$\lg G^* = 0.78625 \lg \omega + 1.54194$	0.99901
20% BRA/5% nano-SiO ₂ composite-modified asphalt	40	$\lg G^* = 0.80582 \lg \omega + 4.46725$	0.99836
	52	$\lg G^* = 0.76273 \lg \omega + 3.96839$	0.99277
	64	$\lg G^* = 0.75282 \lg \omega + 3.33177$	0.99131
	76	$\lg G^* = 0.67665 \lg \omega + 3.03513$	0.99677
25% BRA/5% nano-SiO ₂ composite-modified asphalt	88	$\lg G^* = 0.74308 \lg \omega + 2.15429$	0.99390
	40	$\lg G^* = 0.68216 \lg \omega + 5.06413$	0.99269
	52	$\lg G^* = 0.76603 \lg \omega + 4.55691$	0.99164
	64	$\lg G^* = 0.82397 \lg \omega + 3.86129$	0.99365
30% BRA/5% nano-SiO ₂ composite-modified asphalt	76	$\lg G^* = 0.81728 \lg \omega + 3.17803$	0.99243
	88	$\lg G^* = 0.75088 \lg \omega + 2.51576$	0.99678
	40	$\lg G^* = 0.71391 \lg \omega + 5.43853$	0.99263
	52	$\lg G^* = 0.75119 \lg \omega + 4.80385$	0.99962
30% BRA/5% nano-SiO ₂ composite-modified asphalt	64	$\lg G^* = 0.80121 \lg \omega + 4.12576$	0.99850
	76	$\lg G^* = 0.76467 \lg \omega + 3.36815$	0.99271
	88	$\lg G^* = 0.69195 \lg \omega + 2.73792$	0.99372

Table 7. Summary of displacement factors of modified asphalt.

Types of Modified Asphalt	Testing Temperature (°C)	$\lg\omega$ ($G^* = 1 \text{ kPa}$, rad/s)	Shift Factors
5% nano-SiO ₂ -modified asphalt	40	−1.4476	0
	52	−0.5269	−0.9207
	64	0.3547	−1.8024
	76	1.1638	−2.6115
	88	1.8544	−3.3021
20% BRA/5% nano-SiO ₂ composite-modified asphalt	40	−1.8208	0
	52	−1.2696	−0.5512
	64	−0.4407	−1.3801
	76	−0.0519	−1.7689
	88	1.1381	−2.9589
25% BRA/5% nano-SiO ₂ composite-modified asphalt	40	−3.0259	0
	52	−2.0324	−0.9934
	64	−1.0453	−1.9806
	76	−0.2178	−2.8080
	88	0.6449	−3.6708
30% BRA/5% nano-SiO ₂ composite-modified asphalt	40	−3.4157	0
	52	−2.4013	−1.0144
	64	−1.4051	−2.0107
	76	−0.4814	−2.9343
	88	0.3788	−3.7945

(2) Principal curve analysis

Based on the computed displacement factors for various asphalt types, the five asphalts are shifted to the left to derive the complex modulus master curve at the reference temperature of 40 °C, depicted in Figure 6.

**Figure 6.** Summary of the master curve of complex modulus of five kinds of asphalt.

Observing Figure 6, we can get:

The matrix asphalt exhibits a notably low complex modulus under conditions of elevated temperature and low frequency, implying inadequate resistance to high-temperature

deformation. For equivalent angular frequencies, the modified asphalt showcases a higher complex modulus than the matrix asphalt, signifying the effective enhancement of asphalt’s high-temperature performance through the incorporation of Buton rock asphalt and nano-silica. In comparison to modified asphalt with varying compositions, the complex modulus of Buton rock asphalt/nano-silica composite-modified asphalt surpasses that of nano-silica-modified asphalt. Furthermore, an augmentation in the content of Buton rock asphalt corresponds to an increment in the complex modulus of the composite-modified asphalt. This observation underscores that the inclusion of Buton rock asphalt leads to a heightened enhancement in the high-temperature shear resistance of the asphalt. Moreover, the amplification in the content of Buton rock asphalt accentuates this improvement effect.

Under conditions of low temperature and high frequency, the complex modulus of all five asphalt types rises with an escalation in angular frequency. Notably, the complex modulus of these five asphalt varieties demonstrates a tendency to approach one another, suggesting a certain degree of similarity. The relationship between the complex modulus of the five kinds of asphalt is 30% BRA/5% nano-SiO₂ composite-modified asphalt > 25% BRA/5% nano-SiO₂ composite-modified asphalt > 20% BRA/5% nano-SiO₂ composite-modified asphalt > 5% nano-SiO₂-modified asphalt > matrix asphalt. This observation indicates that, even in low-temperature and high-frequency conditions, the incorporation of Buton rock asphalt and nano-silica remains efficacious in significantly improving the high-temperature performance of the asphalt. As a result, the asphalt demonstrates commendable resistance to deformation.

(3) Multiple stress creep recovery test (MSCR)

The test results of four types of modified asphalt are shown in Figure 7.

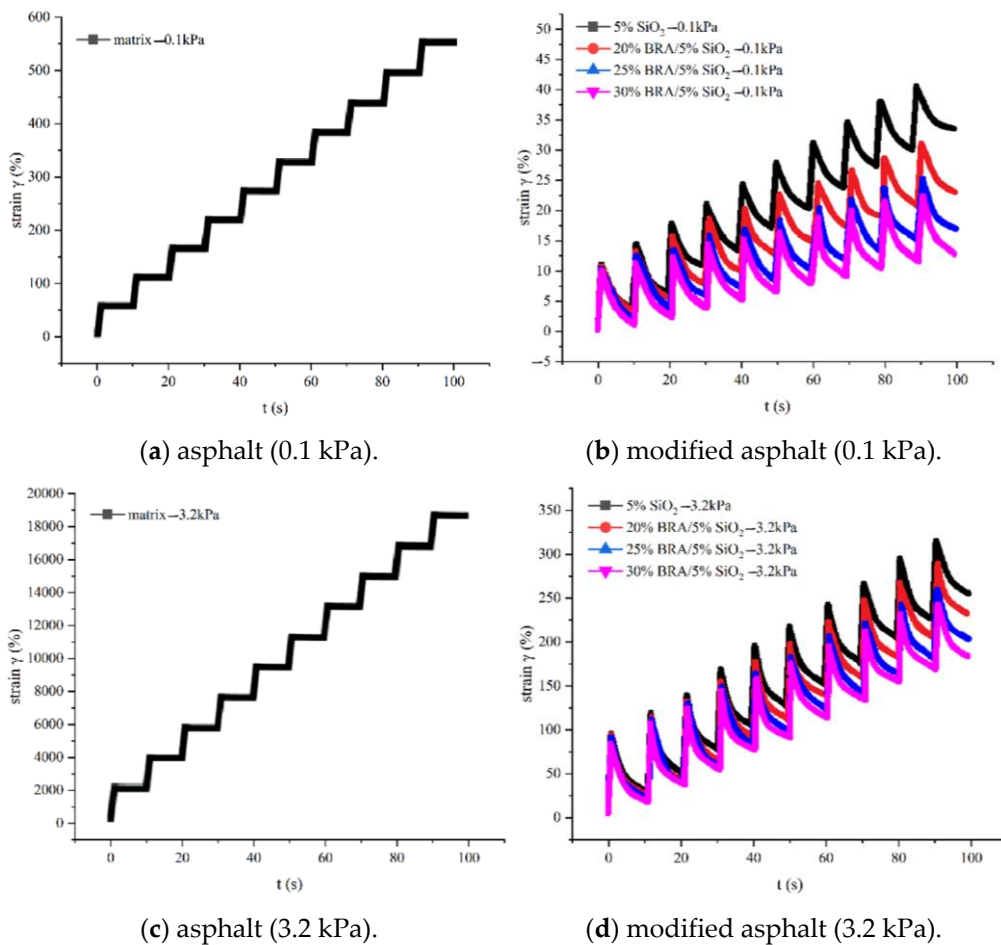


Figure 7. Multi-stress creep recovery test results.

Analyzing Figure 7a,c, it is evident that at the temperature of 64 °C, the strain–time curve of the matrix asphalt exhibits a right angle during each creep cycle at stress levels of 0.1 kPa and 3.2 kPa. This pattern suggests that the matrix asphalt has almost no unloading recovery strain and accumulates a considerable irrecoverable strain, surpassing that of the modified asphalt by a significant margin. From Figure 7b,d, it can be seen that under the two stress levels of 0.1 kPa and 3.2 kPa, the cumulative strain of nano-silica-modified asphalt is greater than the cumulative strain of Buton rock asphalt/nano-silica composite-modified asphalt with different Buton rock asphalt content. With the increase in the content of Buton rock asphalt, a noticeable reduction in the cumulative strain of the composite-modified asphalt becomes evident. This trend indicates that the inclusion of Buton rock asphalt contributes to an enhanced high-temperature deformation resistance of the composite-modified asphalt. Moreover, as the Buton rock asphalt content continues to rise, this enhancement effect becomes increasingly pronounced.

To provide a more comprehensive representation of asphalt’s creep recovery performance, R and Jnr of the five asphalt types are individually calculated at stress levels of 0.1 kPa and 3.2 kPa. These outcomes are visually depicted in Figure 8.

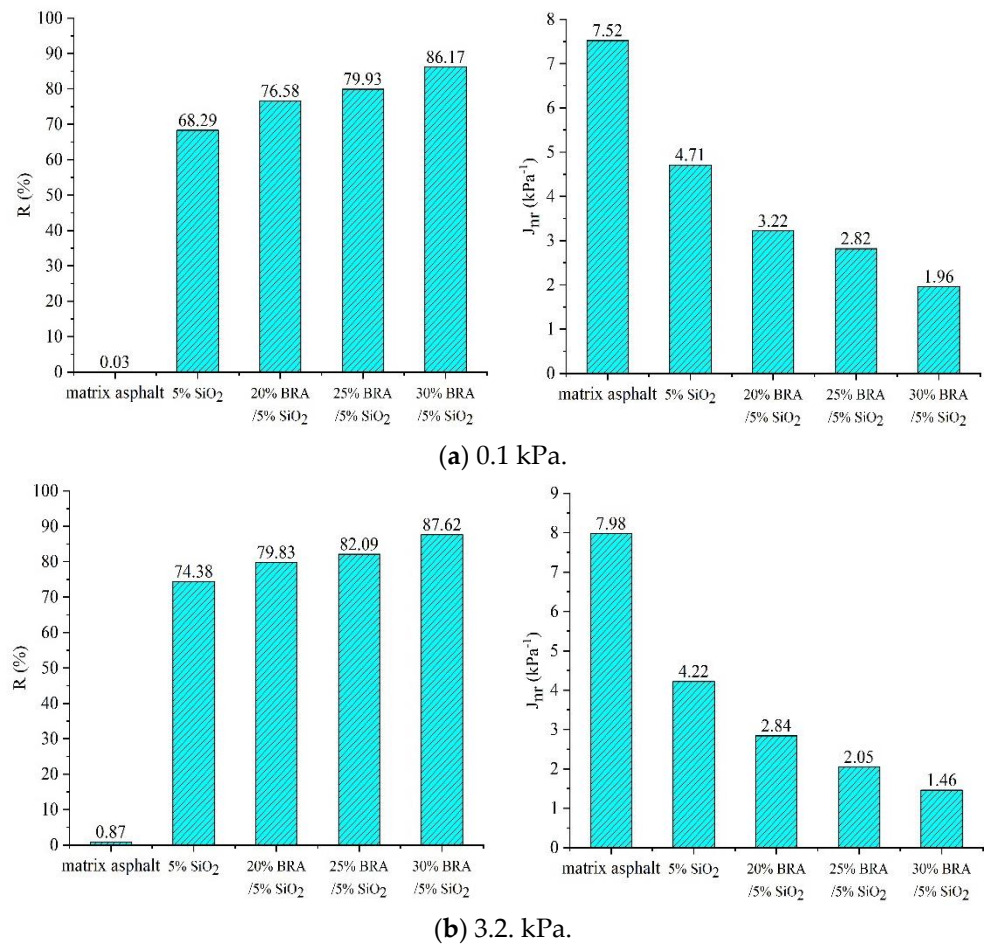


Figure 8. Average creep recovery rate R and non-recoverable creep compliance Jnr of the five kinds of asphalt.

Figure 8 reveals that the strain recovery rates R (0.1) and R (3.2) for the matrix asphalt are nearly 0, indicating a notably low proportion of the elastic component within the matrix asphalt. The unrecoverable creep compliance Jnr0.1 and Jnr3.2 of the matrix asphalt are 7.52 kPa⁻¹ and 7.98 kPa⁻¹, respectively. The non-recovery strain of deformation in the matrix asphalt is higher than that of the modified asphalt, and the recovery ability from deformation is extremely poor. Under the two stress levels of 0.1 kPa and 3.2 kPa, the

strain recovery rate R of modified asphalt is as follows: 30% Buton rock asphalt/5% nano-silica composite-modified asphalt > 25% Buton rock asphalt/5% nano-silica composite-modified asphalt > 20% Buton rock asphalt/5% nano-silica composite-modified asphalt > 5% nano-silica-modified asphalt > matrix asphalt. With Buton rock asphalt content at 30% and nano-silica content at 5%, the $R(0.1)$ and $R(3.2)$ values of the composite-modified asphalt are 26.2% and 17.8% higher, respectively, than those of the nano-silica-modified asphalt. The irrecoverable creep compliance J_{nr} of the modified asphalt is as follows: 30% Buton rock asphalt/5% nano-silica composite-modified asphalt < 25% Buton rock asphalt/5% nano-silica composite-modified asphalt < 20% Buton rock asphalt/5% nano-silica composite-modified asphalt < 5% nano-silica-modified asphalt < matrix asphalt. At a Buton rock asphalt content of 30% and a nano-silica content of 5%, the $J_{nr0.1}$ and $J_{nr3.2}$ of the composite-modified asphalt reach the minimum values of 1.96 kPa^{-1} and 1.46 kPa^{-1} , which are 58.3% and 65.3% lower than those of nano-silica-modified asphalt. The fluctuations observed in the two indices of R and J_{nr} highlight the exceptional creep recovery capability of the Buton rock asphalt/nano-silica composite-modified asphalt. Notably, as the content of Buton rock asphalt increases, the creep recovery ability further improves, underscoring the outstanding high-temperature rutting resistance exhibited by the asphalt pavement.

4.2. Bending Creep Stiffness (BBR) Test

When asphalt is used in areas below 10°C , it is easy to become brittle due to low temperatures [39]. Under the dual impact of low temperature and external loads, shrinkage cracks appear, affecting asphalt pavement's lifespan. Hence, asphalt requires robust low-temperature crack resistance to counter this.

To assess the low-temperature crack resistance of asphalt, SHRP intends to evaluate it using the stiffness modulus (S value) and the creep rate (m value) derived from the Bending Beam Rheometer (BBR) test [40]. The stiffness modulus S value signifies the capacity to withstand load-induced deformation under varying temperatures and loads. A smaller S value indicates better flexibility of the asphalt at low temperatures. Simultaneously, the creep rate (m value) illustrates the rate of change in the stiffness modulus (S value) with temperature variations. A higher m value implies reduced susceptibility to low-temperature stress, thereby minimizing the risk of low-temperature cracking.

According to the test procedure [38], BBR tests were carried out on five groups of asphalt samples, including matrix asphalt, 5% nano- SiO_2 -modified asphalt, 20%, 25%, and 30% composite-modified asphalt with 5% nano- SiO_2 . The test temperature is -12°C , -18°C , and -24°C . To ensure favorable low-temperature crack resistance of the asphalt, the Superpave specification mandates that $S \leq 300 \text{ MPa}$ and $m \geq 0.3$ at 60 s. The creep stiffness modulus S -temperature curve and the creep rate m -temperature curve are depicted in Figures 9 and 10, respectively.

Test outcomes reveal that, under three distinct low-temperature conditions, the creep stiffness modulus of nano- SiO_2 -modified asphalt and BRA/nano- SiO_2 composite-modified asphalt is inferior to that of matrix asphalt. When 5% nano- SiO_2 is added alone, the decrease is the largest. When 5% nano- SiO_2 is added alone, the decrease is the largest. The creep stiffness modulus S at -12°C , -18°C , and -24°C decreased by 52.9 MPa, 179.5 MPa, and 445.9 MPa, respectively. The creep stiffness modulus at -24°C was 286.7 MPa, which was less than the 300 MPa required by the specification. The creep stiffness modulus (S) signifies the flexibility of asphalt at low temperatures. The inclusion of Buton rock asphalt in composite-modified asphalt increases the creep stiffness modulus, thereby improving stress relaxation and low-temperature crack resistance, aided by nano- SiO_2 . It is crucial to acknowledge that the introduction of Buton rock asphalt does lead to a certain reduction in the low-temperature crack resistance of the asphalt.

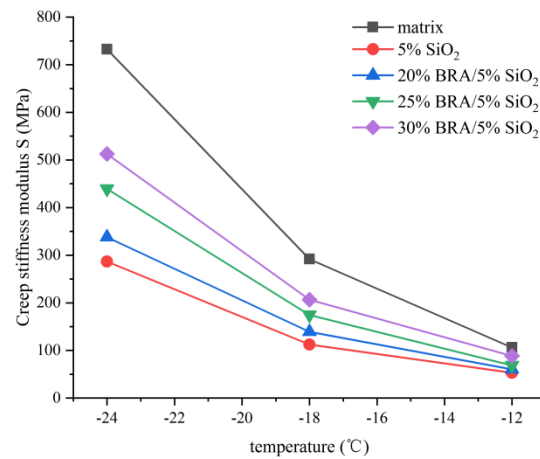


Figure 9. Creep stiffness modulus–temperature curve.

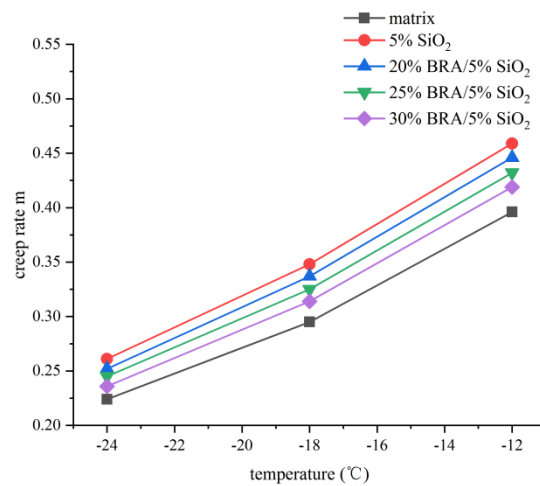


Figure 10. Creep rate–temperature curve.

The creep rate m of nano-SiO₂-modified asphalt and BRA/nano-SiO₂ composite-modified asphalt decreases with the decrease of temperature. Both nano-SiO₂-modified asphalt and BRA/nano-SiO₂ composite-modified asphalt exhibit higher creep rates than matrix asphalt at the same low temperature. At -18 °C, the creep rate m of 5% nano-SiO₂-modified asphalt, 20%, 25%, 30% nano-SiO₂-modified asphalt, and 5% nano-SiO₂-modified asphalt is 18.0%, 14.2%, 10.2%, 6.4% higher than that of matrix asphalt. The creep rate m represents the probability of low-temperature stress. The incorporation of nano-SiO₂ makes it difficult for asphalt to produce temperature stress at low temperatures. The incorporation of Buton rock asphalt makes it easier to produce temperature stress in asphalt, subsequently influencing the asphalt's resistance to low-temperature cracking.

Analyzing the creep stiffness modulus S and creep rate m reveals that the introduction of nano-SiO₂ enhances asphalt's low-temperature crack resistance, while the inclusion of Buton rock asphalt impacts the asphalt's low-temperature crack resistance. Taking all factors into account, when the composite-modified asphalt contains 25% Buton rock asphalt and 5% nano-silica, the resulting mixture exhibits excellent high-temperature performance and a certain degree of improved low-temperature performance.

4.3. Morphology Characterization Analysis of Composite-Modified Asphalt

The microscopic test image of matrix asphalt magnified by 15,000 times is shown in Figure 11.

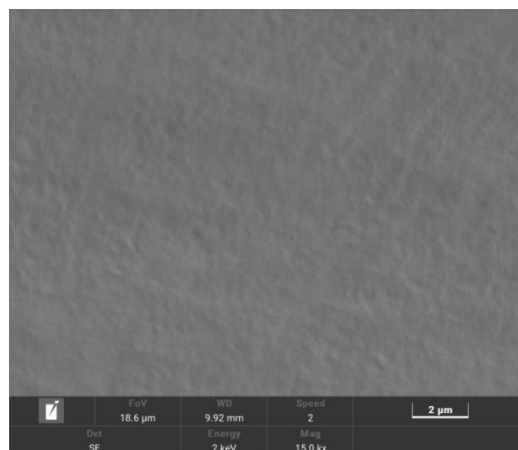


Figure 11. Electron microscopy of base asphalt.

As depicted in Figure 11, the matrix asphalt is magnified by a factor of 15,000, and no particle impurities are observed in the asphalt, which shows the characteristics of smooth and pure as a whole. This shows that the 70# road petroleum asphalt used in the test is pure and reliable, which is convenient to compare with the microstructure of Buton rock asphalt/nano-silica composite-modified asphalt.

The microscopic test image of Buton rock asphalt/nano-silica composite-modified asphalt is enlarged by 15,000 times, as shown in Figure 12.

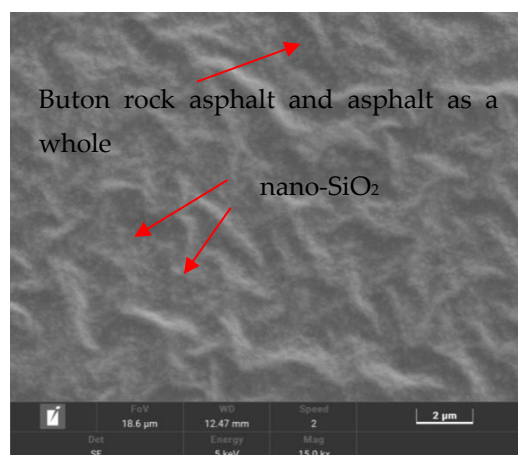


Figure 12. Electron microscopy of nano-SiO₂/BRA compound-modified asphalt.

From Figure 12, it can be seen that the Buton rock asphalt/nano-silica composite-modified asphalt is magnified by 15,000 times, the white dot material is nano-SiO₂, the white continuous phase is a structural whole composed of nano-SiO₂ and asphalt, and the black block area is Buton rock asphalt and asphalt as a whole [29]. Observations indicate the uniform distribution of nano-SiO₂ within the asphalt, attributed to the high-speed shearing process. Nano-SiO₂ belongs to the nano-size range, nano-SiO₂, and asphalt are fully integrated together, and a large part of nano-SiO₂ is wrapped by asphalt. There is no interface layering in the composite-modified asphalt, which indicates that the bonding between the substances is good. This phenomenon arises from the minute dimensions and expansive specific surface area of nano-SiO₂ particles. The activity of the existing particles has a high adsorption on the substances it contacts. The observation reveals a uniform dispersion of the medium, giving rise to a stable network structure through co-adsorption. Additionally, a polymerization effect occurs within the asphalt. This specially formed structure plays a pivotal role in transmitting and dissipating stress when the modified asphalt undergoes external and temperature-related stresses. The existence of nano-SiO₂

can produce stress concentration, micro-cracks appear around, and absorb the stress and energy of asphalt so that the asphalt shows good high and low-temperature performance and temperature sensitivity.

Due to its special “double-sided” structure, Budun rock asphalt melts at high temperatures, and its internal ash particles have been completely wrapped in asphalt, which contacts with nanoparticles and asphalt molecules, combines and interleaves. This overall structure has good support and stability. The ash particles inside this structure interlace each other to strengthen the rigidity of asphalt. The formation of the structure promotes the excellent combination and connection of nano-SiO₂ and asphalt molecules. The continuous phase formation impedes asphalt flow at high temperatures and prevents asphalt shrinkage deformation at low temperatures. The skeleton structure composed of nano and ash particles enhances the anti-bearing capacity of asphalt, leading to improved shear resistance and high/low-temperature performance in composite-modified asphalt.

4.4. Infrared Spectrum Test Analysis of Modified Asphalt

In this paper, the infrared spectrum (IR) test is carried out with a scanning range of 4000–400 cm⁻¹, a resolution of 0.4 cm⁻¹, and 64 scanning times. The infrared spectra of 5% silane coupling agent KH-550 modified nano-silica and untreated nano-silica are shown in Figure 13.

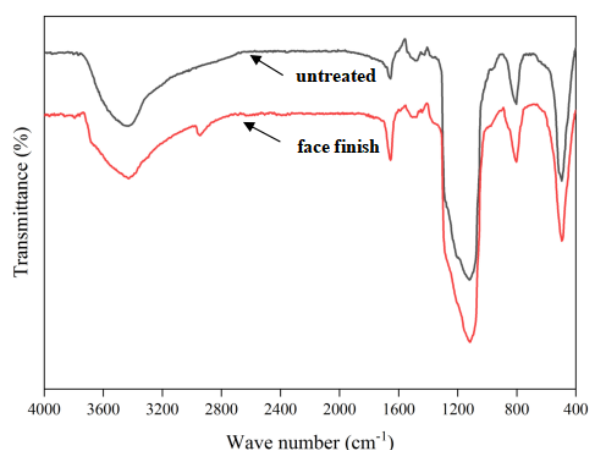


Figure 13. Infrared spectra of nano-silica before and after surface modification.

Figure 13 depicts the infrared spectra of both untreated nano-SiO₂ and surface-modified nano-SiO₂. The wide absorption peak at about 3427.6 cm⁻¹ in the infrared spectrum is the Si-OH stretching vibration peak of water hydroxyl (-OH) adsorbed on the surface of nano-SiO₂, and about 1653.9 cm⁻¹ is the bending vibration peak of water hydroxyl Si-OH adsorbed on the surface of nano-SiO₂. The antisymmetric stretching vibration peak of Si-O-Si appears at about 1118.5 cm⁻¹, the symmetric stretching vibration peak of Si-O-Si appears at about 802.8 cm⁻¹, and the bending vibration peak of Si-O-Si appears at about 496.3 cm⁻¹. These three peaks are the characteristic absorption peaks of nano-SiO₂.

As observed in Figure 13, the absorption spectrum curves of untreated nano-SiO₂ and surface-modified nano-SiO₂ are fundamentally similar. Compared with the untreated nano-SiO₂, the surface-modified nano-SiO₂ has a weaker absorption peak at 3427.6 cm⁻¹ than the untreated nano-SiO₂, which represents that the surface adsorption of nano-SiO₂ modified by silane coupling agent KH-550. The amount of water and the number of Si-OH groups decreased; a new peak at 2945.1 cm⁻¹ appeared on the surface-modified nano-SiO₂, which represented the antisymmetric stretching vibration peak of methyl (-CH₃) and methylene (-CH₂) of silane coupling agent KH-550. Consequently, based on the infrared spectrum analysis, it is deduced that the chemical bond of the silane coupling agent KH-550 is indeed bonded with the surface of nano-SiO₂, and the reaction appears to be thorough

and adequate. The surface of nano-SiO₂ is 'grafted' successfully, and the nano-SiO₂ changes from inorganic to organic, which is easier to fuse with asphalt.

The infrared spectrum (IR) test of the composite-modified asphalt was also carried out with a scanning range of 4000–400 cm⁻¹, a resolution of 0.4 cm⁻¹, and a scanning number of 64 times. In order to facilitate the comparative analysis, the infrared spectra of the composite-modified asphalt and the matrix asphalt are drawn together. Figure 14 displays the infrared spectra of the composite-modified asphalt with 25% content of Buton rock asphalt and 5% content of nano-silica, alongside the infrared spectrum of the matrix asphalt.

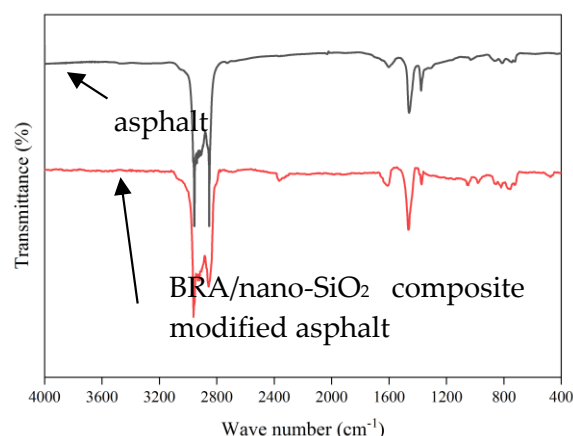


Figure 14. Infrared spectra of two kinds of modified asphalt.

As evident in Figure 14, the absorption peak of Buton rock asphalt/nano-silica composite-modified asphalt and matrix asphalt at approximately 2960.26 cm⁻¹ corresponds to the antisymmetric stretching vibration peak of methyl (-CH₃) and methylene (-CH₂), indicating the stretching vibration of the C-H bond on the benzene ring. The absorption peak at about 1608.34 cm⁻¹ represents the vibration peak of the benzene ring skeleton. The absorption peaks at 1463.71 cm⁻¹ and 1376.85 cm⁻¹ denote the antisymmetric and symmetric bending vibrations of methyl (-CH₃) or methylene (-CH₂), representing the saturated hydrocarbon structure in asphalt molecules. The absorption peak around 1049.09 cm⁻¹ is the symmetrical stretching vibration peak of S = 0, which represents the sulfur functional group of sulfoxide structure in asphaltene. Multiple absorption peaks in the range of 690–870 cm⁻¹ are aromatic C-H out-of-plane bending vibrations, representing aromatic compounds in asphalt.

Compared with the matrix asphalt, the absorption peak of the composite-modified asphalt is roughly all the nano-SiO₂. The new absorption peak at 979.66 cm⁻¹ represents the Si-O-CH₂ bond of the silane coupling agent KH-550, indicating that the coupling agent KH-550 group is still on the nano-SiO₂ molecule after the composite-modified asphalt is prepared by high-speed shearing. Buton rock asphalt has no chemical reaction with asphalt, and the material is mainly physical blending.

5. Conclusions

(1) Incorporating Buton rock asphalt and nano-silica significantly enhances the complex shear modulus G^* of the composite-modified asphalt while reducing the phase angle δ . The rutting factor $G^*/\sin\delta$ also experiences a substantial increase. When compared to the matrix asphalt, the composite-modified asphalt containing 30% Buton rock asphalt and 5% nano-silica exhibits a remarkable enhancement: a 9.41 kPa rise in complex shear modulus G^* at 70 °C, a 29.42° decrease in phase angle δ , and an 11.11 kPa increase in rutting factor $G^*/\sin\delta$. The frequency scanning master curve is at a high level at 64 °C. The matrix asphalt almost completely loses its creep recovery ability at 0.1 kPa and 3.2 kPa stress levels. Both nano-silica-modified asphalt and Buton rock asphalt/nano-silica composite-

modified asphalt exhibit superior high-temperature deformation resistance compared to the matrix asphalt.

Furthermore, the high-temperature performance of the composite-modified asphalt exhibits a continuous enhancement with the increasing content of Buton rock asphalt. Specifically, when the content of Buton rock asphalt is at 30% and the content of nano-SiO₂ is at 5%, the rutting resistance of the composite-modified asphalt reaches its peak strength. The incorporation of both Buton rock asphalt and nano-SiO₂ contributes significantly to the improvement of the asphalt's high-temperature performance.

(2) Across different low temperatures, both nano-silica-modified asphalt and Buton rock asphalt/nano-silica composite-modified asphalt showed a reduction in the creep stiffness modulus (S) compared to matrix asphalt. The inclusion of nano-silica contributes to enhanced stress relaxation performance of asphalt at low temperatures, resulting in a significant improvement in low-temperature crack resistance. Additionally, the creep rate (m) of nano-silica-modified asphalt was higher than that of matrix asphalt. In contrast to the matrix asphalt, the creep stiffness modulus S of 5% nano-silica-modified asphalt decreased by 61.5% at −18 °C, and the creep rate m increased by 18.0% at −18 °C, suggesting the introduction of nano-silica. At lower temperatures, asphalt is less prone to produce temperature stress, resulting in an improved resistance to low-temperature cracking. In comparison to the matrix asphalt, the creep stiffness modulus (S) at −18 °C decreased by 40.2%, and the creep rate (m) at −18 °C increased by 10.2% with the incorporation of Buton rock asphalt. The presence of Buton rock asphalt renders the asphalt more susceptible to temperature stress, thereby influencing its low-temperature performance.

(3) Nano-silica is uniformly dispersed throughout the asphalt. After surface modification, nano-silica is easy to combine with asphalt. Due to the existence of natural asphalt in the composition, buton rock asphalt and matrix asphalt together constitute the whole asphalt system. The overall structure has a good supporting effect and stability. Buton rock asphalt/nano-silica composite-modified asphalt shows superior bearing capacity and high and low-temperature performance.

(4) The antisymmetric stretching vibration peaks of methyl (−CH₃) and methylene (−CH₂) appeared in about 2960.26 cm^{−1} of Buton rock asphalt/nano-silica composite-modified asphalt and matrix asphalt, and the infrared spectra of the two kinds of asphalt were roughly the same. The appearance of the Si-O-CH₂ bond of silane coupling agent KH-550 represents the KH-550 group in asphalt. In general, the absorption spectra and curves of Buton rock asphalt/nano-silica composite-modified asphalt and matrix asphalt are not much different, indicating that nano-SiO₂ has a chemical reaction in asphalt, but this reaction is not strong. Buton rock asphalt has no chemical reaction with asphalt, and the material is mainly physical blending.

Author Contributions: Writing—original draft preparation, C.L., Z.L. and S.J.; writing—review and editing, T.G., Y.C. and S.J.; investigation, J.W. and L.J.; discussion, C.L., T.G. and Y.C. All authors have read and agreed to the published version of the manuscript.

Funding: This work was supported by Key R&D and Promotion of Special Scientific and Technological Research Projects of Henan Province: [Grant Number 182102210061].

Institutional Review Board Statement: Not applicable.

Informed Consent Statement: Not applicable.

Data Availability Statement: Some or all data, models, or codes that support the findings of this study are available from the corresponding author upon reasonable request.

Conflicts of Interest: The authors declare that Henan Transportation Research Institute Co., Ltd. and Xi'an Changda Highway Engineering Inspection Center Co., Ltd. was not involved in the study design, collection, analysis, interpretation of data, the writing of this article or the decision to submit it for publication. The authors declare no conflict of interest.

References

1. Li, P. Research on construction quality control of asphalt pavement. *Transp. Manag. World* **2022**, *24*, 10–12.
2. Wang, F. Analysis of the influence of different kinds of modifiers on the performance of matrix asphalt. *Appl. Chem. Ind.* **2021**, *50*, 2132–2135+2139. [[CrossRef](#)]
3. Chen, Q.; Li, Y.; Wang, C.; Feng, L.; Zhang, Z. Degradation of mechanical properties of polyurethane elastomer coatings under different pavement pollution conditions. *Constr. Build. Mater.* **2023**, *409*, 134181. [[CrossRef](#)]
4. Wang, Y. Application research status of nano modified asphalt materials in pavement engineering. *Aging Appl. Synth. Mater.* **2022**, *51*, 159–161. [[CrossRef](#)]
5. Yang, X. Nano-silica and its application status and development prospect. *Inn. Mong. Petrochem. Ind.* **2011**, *37*, 26–27.
6. Shafabakhsh, G.; Sadeghnejad, M.; Ebrahimi, R. Fracture resistance of asphalt mixtures under mixed-mode I/II loading at low-temperature: Without and with nano SiO₂. *Constr. Build. Mater.* **2021**, *266*, 120954. [[CrossRef](#)]
7. Yadykova, A.Y.; Ilyin, S.O. Rheological and adhesive properties of nanocomposite bitumen binders based on hydrophilic or hydrophobic silica and modified with bio-oil. *Constr. Build. Mater.* **2022**, *342*, 127946. [[CrossRef](#)]
8. Cheraghian, G.; Wistuba, M.P. Effect of Fumed Silica Nanoparticles on Ultraviolet Aging Resistance of Bitumen. *Nanomaterials* **2021**, *11*, 454. [[CrossRef](#)] [[PubMed](#)]
9. Lu, X.; Zhang, S.; Wu, Y. Effect of Budun rock aggregate on the performance of asphalt mixture. *J. Build. Mater.* **2015**, *18*, 450–457.
10. Tang, Y.; Ling, L.; Lu, W.; Zhang, H.; Zhao, Q. Study on Performance Test and Road Use Value of BRA Modified Asphalt Mixture. *Heilongjiang Transp. Sci. Technol.* **2023**, *46*, 45–47. [[CrossRef](#)]
11. Zhang, Z. Research on Performance of BRA Modified Asphalt. *IOP Conf. Ser. Earth Environ. Sci.* **2021**, *719*, 022086. [[CrossRef](#)]
12. Zhou, Z. Study on Rheological Properties of BRA Modified Asphalt. *IOP Conf. Ser. Earth Environ. Sci.* **2019**, *330*, 042030. [[CrossRef](#)]
13. Li, R.X.; Hao, P.W.; Wang, C. Performance Evaluation of BRA Modified Asphalt Based on Analysis of Rheological Property. *Adv. Mater. Res.* **2011**, *374–377*, 1385–1390. [[CrossRef](#)]
14. Muhammad, K.; Ainalam, N.; Ahdyeh, M.; Hamid, N. Evaluation of Permanent Deformation of BRA Modified Asphalt Paving Mixtures Based on Dynamic Creep Test Analysis. *Adv. Eng. Forum* **2016**, *4416*, 69–81. [[CrossRef](#)]
15. Bo, S. Study on preparation and properties of High viscosity elastic restored asphalt. *Highw. Automob. Transp.* **2023**, *2*, 49–52+72. [[CrossRef](#)]
16. Wu, Y.; Liao, J.; Huang, W.; Feng, W.; Cao, M. High temperature performance analysis of Buton rock asphalt modified asphalt. *J. Chengdu Univ.* **2019**, *38*, 106–110.
17. Wang, M.; Lin, F.; Liu, L. Dynamic rheological properties and microscopic characteristics of Buton rock asphalt ash mortar. *J. Tongji Univ.* **2016**, *44*, 567–571.
18. Zhou, C.; Zhang, S.; Guan, Y.; Zhou, W. Research on improving the performance of matrix asphalt slurry with high ash natural rock asphalt. *Highw. Transp. Technol. (Appl. Technol. Ed.)* **2016**, *12*, 44–46.
19. Lei, M.; Fei, Y. Research on application of rock asphalt high strength mixture BRAC-16 in cold region. *Shanxi Archit.* **2017**, *43*, 112–113. [[CrossRef](#)]
20. Yang, Y.; Huang, P.; Zhou, W.; Liu, H.; Fei, Y. High ash rock asphalt modified asphalt mixture road performance and its mechanism of action. *Highw. Transp. Technol. (Appl. Technol. Ed.)* **2019**, *15*, 22–25.
21. Gholam, A.S.; Mostafa, S.; Behzad, A.; Esmail, T. Laboratory experiment on the effect of nano SiO₂ and TiO₂ on short and long-term aging behavior of bitumen. *Constr. Build. Mater.* **2020**, *237*, 117640. [[CrossRef](#)]
22. Sun, L.; Xin, X.; Ren, J. Inorganic Nanoparticle-Modified Asphalt with Enhanced Performance at High Temperature. *J. Mater. Civ. Eng.* **2016**, *29*, 04016227. [[CrossRef](#)]
23. Zhu, W. Effect of nano-silica content on the performance of asphalt mixture. *Contemp. Chem. Ind.* **2019**, *48*, 2553–2556. [[CrossRef](#)]
24. Sun, L.; Xin, X.; Yu, P. Pavement performance of nano-SiO₂ modified asphalt mixture. *Highw. Traffic Technol.* **2013**, *30*, 1–5.
25. Yang, Y.S.; Fan, W.Y.; Wang, Z.; Zhang, Q.Q.; Nan, G.Z. Effect of Nano SiO₂ on the Performance of Asphalt Emulsion and its Residue. *Adv. Mater. Res.* **2011**, *413*, 331–335. [[CrossRef](#)]
26. Mehmet, S.; Serdal, T.; Sebnem, K. Examination of hot mix asphalt and binder performance modified with nano silica. *Constr. Build. Mater.* **2017**, *156*, 976–984. [[CrossRef](#)]
27. He, H.; Hu, J.; Li, R.; Shen, C.; Pei, J.; Zhou, B. Study on rheological properties of silica nanofluids modified asphalt binder. *Constr. Build. Mater.* **2021**, *273*, 122046. [[CrossRef](#)]
28. Yue, C.; Gao, D.; Wang, Y.; He, W.; Fu, L.; Liu, C.; Li, Z.; Cheng, F. Preparation and properties evaluation of micro-nano SiO₂ modified asphalt. *Fine Chem. Ind.* **2023**, *40*, 2302–2311. [[CrossRef](#)]
29. Tan, Y. Study on properties of oil-wet nano-silica modified asphalt. *Transp. Sci. Technol.* **2023**, 108–114.
30. Zhang, H.; Zhu, C.; Zhang, B.; Yu, J. Effects of surface modified nano-silica on asphalt properties. *J. Build. Mater.* **2014**, *17*, 172–176.
31. Long, Z.; Zhou, S.; Jiang, S.; Ma, W.; Ding, Y.; You, L.; Tang, X. Revealing compatibility mechanism of nanosilica in asphalt through molecular dynamics simulation. *J. Mol. Model.* **2021**, *27*, 81. [[CrossRef](#)] [[PubMed](#)]
32. Long, Z.; Tang, X.; Guo, N.; Ding, Y.; Ma, W.; You, L.; Xu, F. Atomistic-scale investigation of self-healing mechanism in Nano-silica modified asphalt through molecular dynamics simulation. *J. Infrastruct. Preserv. Resil.* **2022**, *3*, 4. [[CrossRef](#)]
33. Khordehbinan, M.; Fakhrefatemi, S.-M.-R.; Ghanbari, S.; Ghanbari, M. The effect of nano-SiO₂ and the styrene butadiene styrene polymer on the high-temperature performance of hot mix asphalt. *Pet. Sci. Technol.* **2017**, *35*, 553–560. [[CrossRef](#)]

34. Abed, A.H.; Oudah, A.M. Rheological properties of modified asphalt binder with nanosilica and SBS. *IOP Conf. Ser. Mater. Sci. Eng.* **2018**, *433*, 012031. [[CrossRef](#)]
35. Mostafa, S.; Gholamali, S. Use of Nano SiO₂ and Nano TiO₂ to improve the mechanical behaviour of stone mastic asphalt mixtures. *Constr. Build. Mater.* **2017**, *157*, 965–974.
36. Shafabakhsh, G.H.; Ani, O.J. Experimental investigation of effect of Nano TiO₂/SiO₂ modified bitumen on the rutting and fatigue performance of asphalt mixtures containing steel slag aggregates. *Constr. Build. Mater.* **2015**, *98*, 692–702. [[CrossRef](#)]
37. *T/CECS G: D54-02-2020*; Technical Specification for Application of Buton Bituminous Rock in Road. People's Transportation Press: Beijing, China, 2020.
38. *JTG E20-2011*; Test Code for Asphalt and Asphalt Mixture of Highway Engineering. People's Traffic Press: Beijing, China, 2011.
39. Shao, F. *Study on Preparation Process of SBS Modified Emulsified Asphalt*; East China University of Science and Technology: Shanghai, China, 2021. [[CrossRef](#)]
40. Yin, H.; Li, K. Evaluation of low-temperature performance of asphalt based on bending beam rheological test and viscoelastic theory. *Funct. Mater.* **2021**, *52*, 10157–10165.

Disclaimer/Publisher's Note: The statements, opinions and data contained in all publications are solely those of the individual author(s) and contributor(s) and not of MDPI and/or the editor(s). MDPI and/or the editor(s) disclaim responsibility for any injury to people or property resulting from any ideas, methods, instructions or products referred to in the content.